A theoretical model of neural maturation in the developing spinal cord

Piyush Joshi[1,2], and Isaac Skromne[1,3]*

[1]Department of Biology, University of Miami, 1301 Memorial Drive, Coral Gables, Florida, 33146, United States

[2]Current Address: Cancer and Blood Disorders Institute, Johns Hopkins All Children's Hospital, 600 5th St. S, St. Petersburg, FL 33701

[3]Current Address: Department of Biology, University of Richmond, 28 Westhampton Way B322, Richmond, Virginia, 23173, United States

***Corresponding author:** (I.S.) Tel.: +1-804-829-8235; Fax: +1-804-289-8871; E-mail: iskromne@richmond.edu

Keywords: CDX, neurogenesis, spinal cord, gene regulatory network

Running title: Mathematical model of spinal cord neural maturation

Abstract (251 words)

Cellular differentiation is a tightly regulated process under the control of intricate signaling and transcription factors networks working in coordination. Due to their complexity, these networks are studied and modelled independently despite their codependence: signals instruct transcription factors to drive cellular responses, and transcription factors provide the context for the cells to respond to signals. These reciprocal interactions make the systems dynamic, robust and stable but also difficult to dissect. Differential equation based mathematical models provide an important theoretical tool to understand the behavior of these intricate networks. In the spinal cord, recent work has shown that a network of FGF, Wnt and Retinoic Acid (RA) signaling factors regulate neural maturation by directing the activity of a transcription factor network that contains CDX at its core. Here we have used differential equation based models to understand the spatiotemporal dynamics of the FGF/Wnt/RA and the CDX regulated networks, alone and in combination. We show that in both networks, the strength of interaction among network partners impacts the dynamics, behavior and output of the system. In the signaling network, small changes in the strength of the interactions among networking partners can result in a signal overriding, balancing or oscillating with another signal. We also show that the signaling network conveys the spatiotemporal information to the transcription network, whose interpretation produces a transition zone to separate regions of high cell potency from regions of cell differentiation. This analysis provides a model for the interaction conditions underlying spinal cord cell maturation during embryonic axial elongation.

Introduction

Cells sequentially differentiate from high to low potency states, under the guidance of extracellular signals working in coordination with intracellular transcription factors. Signals regulate the individual and network activity of the transcription factors by providing spatial and temporal information [1-4]. In turn, transcriptional network dictates a cell's competence and response to extracellular signals [5-7]. Because signaling information changes the composition of a cell's transcriptional components, this creates an intricate and dynamic cross-regulatory system for guiding cell differentiation that has been challenging to untangle and comprehend [1, 3, 4].

Vertebrate spinal cord provides an advantageous model to study the cross-regulatory dynamics involved in central nervous system development in particular, and differentiation in general. The head (rostral) to tail (caudal) development of spinal cord during vertebrate body extension results into a characteristic spatial separation of temporal differentiation events [8-10], facilitating the study of their regulation. Briefly, the spinal cord neural progenitors (NPs) are derived from a bipotent population of cells located at the caudal most end of the embryo, the neuro-mesodermal progenitors (NMPs). In the early embryo, the region where NMPs reside is known as the caudal lateral epiblast and node streak border, and in the late embryo, the caudal neural hinge [8-10]. During development, NPs exit the NMP domain rostrally and sequentially transit through different maturation states as they become part of the elongating spinal cord [8, 11, 12].

NP maturation is driven by synergistic and antagonistic interactions between the signaling factors FGF, WNT and Retinoic Acid (RA), turning on and off key transcription factors required for caudal-to-rostral maturation events (**Fig 1A**). Current models propose that two opposite signaling gradients regulate spinal cord cell maturation [13]: from caudal/high to

rostral/low, FGF and WNT gradients prevents cell differentiation by promoting high potency cell states caudally; whereas an opposite rostral/high to caudal/low gradient of RA secreted from somites promotes cell differentiation rostrally. Importantly, FGF and WNT activity gradient counteract RA activity gradient. In this way, cells located caudally experience high levels of FGF/WNT and no RA, which drives expression of bipotency markers *T/Bra*, *Sox2*, and *Nkx1.2* [11, 14, 15]. T/BRA and SOX2 are transcription factors that repress each other and promote different cell fates, with T/BRA promoting mesoderm and SOX2 promoting neural fates [16-19]. In addition, both transcription factors downregulate FGF and Wnt, initiating the early differentiation of mesoderm or neural tissues [16]. NMPs that continue to transcribe *Sox2* but not *T/Bra* assume NPs identity and become part of the growing neural plate. As NPs transit through the maturing neural plate, they experience a further gradual loss in FGF and WNT, and a gradual increase in RA signaling. This new environment lead to the caudal-to-rostral downregulation of a third bipotency marker, *Nkx1.2*, and upregulation of the early differentiation gene *Pax6* [20]. Subsequently, under RA regulation, PAX6 activates late differentiation genes such as *Ngn2* (**Fig 1B**) [10, 21, 22]. We recently mapped the interactions of these transcription factors into a gene regulatory network (GRN) and place it in the context of the FGF/WNT-RA signaling network (**Fig 1C**) [12]. This work identified the transcription factor CDX4 as a core system component essential for the sequential maturation of NPs into mature neuronal precursors (**Fig 1C**).

Fig 1. FGF-WNT-RA signaling results in nested transcription factor expression domains in the caudal spinal cord. (**A**) Schematic representation of the caudal end of a stage HH10-11 chick embryo. Expression domains of *Fgf8* (red) and *Wnt8c* (magenta) signaling factors, and the Retinoic Acid synthesizing enzyme *Raldh2* (blue), are superimposed on the diagram (based on [23]). Expression domain of relevant transcription factors are indicated on the left (based on

[12]). (**B**) Transcript distribution of key transcription factors involved in caudal spinal cord maturation. Scale bar is 200μm. (**C**) Postulated gene regulatory network showing interaction between signaling factors and transcription factors (based on [12, 16, 21, 23]).

Here we use differential equations to dynamically analyze the GRN driving NP maturation during early spinal cord development. As the transcription factor network depends upon inputs form the FGF-WNT-RA signaling network, we first analyzed the postulated effectiveness of the signaling network to work as a signaling switch [23]. We then used the resulting signaling dynamics as input to evaluate the performance of the underlying transcription GRN in its ability to generate cell state patterns similar to those observed in experimental models. Our results show that signaling interaction can give rise to various developmentally observed phenotypes based on a limited subset of interaction parameters, and these behaviors are robust and stable to perturbations. This is due to strong cross-regulation interactions between system elements. Our results suggests that the dominant predictor of the GRN response is the interaction strength among network partners. By outlining the conditions that permit the operation of the GRN during NP maturation *in silico*, the model predicts and informs on cellular behaviors of the system *in vivo*.

Methods

Transcriptional regulation of genes in the interaction network were modeled by differential equations describing the rate of change of mRNA and protein [24-26], as follows

mRNA dynamics:

$$\frac{dM}{dt} = \alpha_m H_1 - \beta_m M H_2$$

Protein dynamics:

$$\frac{dP}{dt} = \alpha_p M H_3 - \beta_p P H_4$$

,where,

α_m = Transcription rate constant. β_m= mRNA decay rate constant. α_p= Translational rate constant. β_p= protein decay rate constant.

M and *P* are mRNA and protein concentrations, respectively.

H_1 , H_2, H_3, H_4; are Hill functions describing regulatory interaction by upstream factors.

Hill function describing activation is of the form:

$$H_i = \frac{\left(\frac{A}{A_c}\right)^n}{1 + \left(\frac{A}{A_c}\right)^n}$$

,where A is the concentration of activator protein, A_c is the Hill constant and *n* is the Hill coefficient of cooperativity.

Multiple activators can be described with the equation

$$H_i = \frac{\left(\frac{A1}{A1_c}\right)^{n1} + \left(\frac{A2}{A2_c}\right)^{n2}}{1 + \left(\frac{A1}{A1_c}\right)^{n1} + \left(\frac{A2}{A2_c}\right)^{n2}}$$

The Hill function describing repression is of the form:

$$H_i = \frac{1}{1 + \left(\frac{R}{R_c}\right)^m}$$

,where R is the concentration of repressor protein, R_c is the Hill constant and m is the Hill coefficient of cooperativity.

Multiple repressors can be described with the equation

$$H_i = \frac{1}{1 + \left(\frac{R1}{R1_c}\right)^{m1} + \left(\frac{R2}{R2_c}\right)^{m2}}$$

Finally, a regulation where both an activator and a repressor act together can be represented with the equation:

AND configuration: Where activator and repressor can bind on separate regulatory regions.

$$H_i = \frac{\left(\frac{A}{A_c}\right)^n}{1 + \left(\frac{A}{A_c}\right)^n} \; x \frac{1}{1 + \left(\frac{R}{R_c}\right)^m}$$

OR configuration (Competitive inhibition): Where activator and repressor competes for a regulatory region.

$$H_i = \frac{\left(\frac{A}{A_c}\right)^n}{1 + \left(\frac{A}{A_c}\right)^n + \left(\frac{R}{R_c}\right)^m}$$

In case of a diffusing molecule, a diffusion term, $\mu \frac{d}{dx^2}$,was added on the left side of the equation (μ is diffusivity coefficient, x is the spatial dimension).

Differential equations representing the interaction network were numerically solved using MATLAB solver. Partial differential equations showing interactions among factor with diffusing molecules were solved using MATLAB *pdepe* solver. Ordinary differential equations were solved using MATLAB *ode45* solver. MATLAB was also used to plot the simulations of the equation systems.

In situ hybridization

Analysis of gene transcription by *in situ* hybridization was done using digoxigenin (DIG)-labeled antisense RNA probes synthesized and hybridized using standard protocol [27], as previously described [12]. Briefly, embryos were harvested at the appropriate stage and fixed with 4% paraformaldehyde diluted in 1x PBS at 4° C overnight. After a series of washes, embryos were exposed overnight in hybridization solution to DIG-labeled antisense RNA probes against *Pax6, Nkx1.2, Bra, Sox2, Cdx4 or Ngn2*. mRNA expression was detected using an Alkaline Phosphatase coupled Anti-DIG antibody (Roche) and developing embryos with nitro-blue tetrazolium salt (NBT, Thermo Scientific) and 5-bromo-4-chloro-3-indolyl-phosphate (BCIP, Biosynth) at room temperature until dark purple precipitate deposited revealing the areas of gene transcription. Post-development, embryos were washed with 1x TBST and then fixed in 4% PFA. Processed embryos were photographed using an AxioCam MRc digital color camera mounted on a on Zeiss V20 Stereo microscope and processed using Adobe Photoshop (CC2017,Adobe) for size and resolution adjustment and figure preparation.

Results

FGF-WNT-RA signaling interaction network can drive signaling switch

In order to model the transcription factor network responsible for spinal cord cell maturation (**Fig 1C**), we first simulated the signaling dynamics between FGF, WNT and RA that drive the system [13, 23]. As several FGF and WNT factors are transcribed within and around the caudal neural plate performing redundant function [23, 28], for simplicity we focused on the factors shown to have the most influence on the system: FGF8 and WNT8C [23]. *Fgf8* is transcribed in the caudal stem zone (**Fig 1A**), where it inhibits *Raldh2* transcription (no RA production), and promotes *Cyp26a* transcription (high RA degradation) [21]. In the caudal stem and transition zone, FGF8 also activates *Wnt8c* transcription [23]. WNT8C then induces *Raldh2* transcription in more rostral tissues, the somites, where it outcompetes FGF8-mediated repression [23]. RA produced by RALDH2 diffuses from the somites into the caudal spinal cord where it inhibits *Fgf8* transcription [21, 29]. Once *Raldh2* induction has occurred, its expression in nascent somites is maintained even in the absence of WNT activity [23]. While the mechanism of R*aldh2* maintenance remains unknown, for simplification, our model assumes a positive autoregulation of *Raldh2* by RA. Together these interactions give rise to an extended negative feedback loop (**Fig 2A**).

Fig 2. FGF-WNT-RA signaling interaction can result into distinct dynamic behaviors. (**A**) Schematic representation of the interaction between FGF8, WNT8C and RA signaling (based on [23]). Italicized lower case name indicate mRNA products and upper case names indicate protein products, except for RA, which indicates production of the metabolite Retinoic Acid. (**B**) Schematic representation showing the spatial domain where signaling interactions were

simulated (x-axes in graphs). The domain shown between dashed vertical lines has a constant length and moves caudally to the left at a constant rate. Initially, the entire domain is undifferentiated (red) but, as time progresses, cell at the rostral end start to differentiate at a rate defined by the simulation (green; right side of diagram). (**C-E**) Representative results obtained after simulations of the signaling network shown in **A** using parameters shown in **Table 1**. Results were categorized into four groups based on the final distribution of FGF8 and RA levels: FGF8 dominant (**C**), FGF-RA balance (**D**), FGF-RA switch (**E**), and RA-oscillations (**Fig S3**). Right graphs shows distribution of FGF8 (red), WNT8C (magenta) and RA (blue) at the end of the simulation (t=6000 min). Middle and right graphs are heat maps that respectively represent the levels of FGF8 and RA in the region of interest (x axes) over simulation time (y axes).

Cell proliferation in the stem zone drives the extension of the vertebrate axis caudally and the differentiation of tissues rostrally [8]. To simulate the tissue's caudal ward movement, the signaling interactions were confined to a caudally moving spatial domain of constant length extending rostrally from the stem cell zone. Thus, from the perspective of the caudal end, the moving spatial domains appears stationary (**Fig 2B**). To simulate the interactions between signaling factors, we used partial differentiation Hill equations, each containing constants for synthesis, degradation, diffusion and interactions strengths that could potentially impact system behavior. For the purpose of our study we focused on varying the interaction parameter, namely the Hill constant, keeping rest of the parameters unchanged. The Hill constant of a given reaction is the concentration of a factor involved in transcription or signaling at which the rate of reaction regulated by the factor is half of the maximum possible rate. Hence, Hill constant is inversely

related to the affinity of a factor for its target and can act as a measure of factor's interaction strength (**Supplemental information, Fig S1**).

To understand all possible behaviors that could originate from the extended FGF-WNT-RA network, we analyzed the system behavior by modulating the input of FGF and/or RA. Interaction strengths were varied from strong (Hill constant =0.1) to weak (Hill constant =100) activator/repressor activity, in various combinations. The model simulates how the system behaves spatially given a set initial value and a graded exponential decay of *Fgf8* transcription, and is based on the caudal movement of the stem zone cells that are the only cells that actively transcribe *Fgf8* [30]. By varying only the interaction strength between FGF, WNT and RA we obtained various temporal signaling information profiles that we grouped into four broad behaviors: FGF-dominant, FGF-RA balance, FGF-RA switch, and RA aberrant/oscillatory.

FGF8 dominance: In a system where FGF8 repression of *Raldh2* transcription outweighs RA repression of *Fgf8* transcription, the interactions do not result in appreciable RA production (e. g., **Table 1-I; Fig 2C, Fig S2A**). Such a system would lead to maintenance of pluripotent stem progenitor cells without differentiation.

Table 1. Examples of some of the Hill constants combinations tested to investigate signaling dynamics behavior

Hill constants	I	II	III	IV	V	VI	VII	VIII
F_{FW} FGF dependent activation of *Wnt8c* transcription	10	10	10	10	10	10	10	10
F_{FR1} FGF dependent repression of *Raldh2* transcription	1	1	5	10	10	10	2	20
F_{FR2} FGF dependent activation of RA degradation (via CYP26A enzymes)	2	10	15	10	10	10	20	20
W_{WR} WNT dependent activation of *Raldh2*	1	1	0.2	0.5	0.2	0.5	1	1

transcription								
R_{RF} RA dependent repression of *Fgf8* transcription	10	1	0.2	0.1	0.3	0.45	1	20
R_{RR} RA dependent activation of *Raldh2* transcription	50	50	50	50	50	50	300	300
Outcome	FGF dominant	FGF-RA balance	FGF-RA switch				RA aberrant/ oscillatory	

FGF8-RA balance: FGF8, WNT8C and RA signaling domains balance each other and settle on a stable steady state profile (**Table 1-II; Fig 2D, Fig S2A, B**). Such steady state is achieved when the activating and repressive interactions of the system have reached an equilibrium. In these conditions, the regions of FGF8 and RA activities are restricted to domains that maintain the same distance from one another as long as they continue to move caudally at the same speed as the stem cell zone.

FGF-RA switch: The most interesting behavior obtained from simulation is where the system starts with an *Fgf8* mRNA gradient and ends with RA activity gradient over the entire spatial domain (**Table 1-III; Fig 2E, Fig S2A**). This behavior simulates a system that starts with a caudally located stem cell zone and a field of undifferentiated cells that is gradually converted, in a rostral to caudal direction, to a field of differentiate cells. Significantly, this is the mechanism by which axial elongation is thought to cease in embryos [31, 32]. The rate at which the FGF8-to-RA transition occurs, and hence differentiation, is also modulated by the strength of mutually repressive FGF-RA interactions (**Table 1-IV through VI**; **Fig 3**).

Fig 3. Strength of RA inputs determine change rate of FGF-RA switch. Temporal changes in RA production (low/blue to high/yellow) at different position in the tissue (x-axis) is dependent

on the strength of WNT8C stimulation (W_{WR}), and FGF8 repression (R_{RF}). (**A**) Fast FGF-RA switch (t<1500 min) results from relatively moderate activation and very strong repression inputs (W_{WR}=0.5, R_{RF}=0.1). (**B**) Intermediate FGF-RA switch (t<3000 min) results from relatively strong activation and moderate repression inputs (W_{WR}=0.2, R_{RF}=0.3). (**C**) Slow FGF-RA switch (t<5500 min) results from moderate activation and repression inputs (W_{WR}=0.5, R_{RF}=0.45).

RA aberrant/oscillatory: Some parameters in the FGF-WNT-RA interaction system lead to an oscillation in RA levels that did not match the behavior of the system *in vivo*. These oscillations occurred when Hill constants for RA inputs were weak, particularly for the RA-dependent activation of *Raldh2* production. In some cases, we also observed an aberrant behavior in which the production of an RA peak was surrounded by areas devoid of RA (**Table 1 VII, VIII**; **Fig S3**).

Altogether, our results show that the FGF8-WNT8C-RA interaction network as postulated by Olivera-Martinez et al. [23] could indeed give rise to a signaling switch that could travel caudally during the elongation of the embryonic axis, potentially regulating axial length. However, the behavior of the switch depends on the interaction parameters, which regulates the position and the rate of the area of cell differentiation.

FGF-WNT-RA signaling switch and transcription factor interactions establish areas of pluripotency, early and late differentiation

To begin simulating the dynamics of the transcription factor network, we integrated the transcription (**Fig 1C**) and signaling (**Fig 2A**) networks into a single supra-network (**Fig 4A**),

and used the FGF-RA balance profile output as the input signaling information (**Fig 2D, 4B**), as it most closely resembles the distribution of signaling activity during the steady state period of embryo growth (**Fig 1A**). The simulation follows the transcriptional profile of cells that are born caudally at t=0 and at subsequent times are displaced rostrally by the appearance of new cells, away from the stem cell zone and the source of FGF and WNT (**Fig 4C**). As FGF/WNT level decrease, RA levels increases as shown in the in the FGF-RA balance profile simulation (**Fig 2D, 4B**). These changes in spatial signal information are the drivers of transcription factors expression. Since these cells are arranged spatially in order of their birth, from caudal to rostral, the temporal changes in transcription factors give rise to spatial changes in profiles.

Fig 4. Transcriptional interaction strengths dictates response and output of network to overlying signaling information. (**A**) Integrated transcription and signaling interaction network. Hypothetical factors X and Y are predicted from experimental data [12]. (**B**) Reference signaling factor input from Fig 2D used for simulations. (**C**) Location of reference cell (circle) within the spatial domain of signaling activity (vertical dashed lines). Cell remains in the location where it was born as spatial domain is displaced caudally. (**D-F**) Transcription profile of cell in with all interactions equally moderate (**D**; Hill constants=20), equally strong (**E**; Hill constants=2), and variable (**F**; as defined in Table 2). Output of simulation in F most closely resembles the spatial distribution of transcription factors observed in embryos (staggered distribution of expression domains). Distribution of gene transcripts from caudal (0 μm) to rostral (2600 μm) end of the spatial domain is represented at the bottom of each graph with colored bars: *Sox2* in dark orange; *T/Bra* in dark blue; *Nkx1.2* in light orange; *Cdx4* in purple; *Pax6* in light blue; and *Ngn2* in maroon.

The transcription output of the system depends on signaling inputs and transcription factor interactions. Signals regulate the transcription factor network at two distinct key points. The first point of regulation is towards the caudal end of the embryo, where FGF8 and WNT8C, alone or in combination, are required for *T (Bra), Sox2, Nkx1.2* and *Cdx4* transcription [14, 33-37]. The second point of regulation is towards the rostral end of the neural plate, where RA is a necessary for the activation of the early differentiation gene *Pax6* by CDX4 [12, 38]. In addition, several transcription factor interactions are also at play, independently of signaling inputs. For example, *Nkx1.2* transcription is negatively regulated by CDX4 and its own NKX1.2 protein [12, 35], which in turn blocks *Pax6* transcription [12, 39]. In contrast, transcription of late differentiation gene *Ngn2* is activated by PAX6 and repressed by CDX4 [12, 22]. Given that CDX4 is an activator and not a repressor [40], our model invokes two putative repressors *X* and *Y* to mediate the indirect repressor activity of CDX4 [12]. These repressors are assumed to be inhibited by FGF8 [12].

Intuitively, the spatial dynamics of the signal interactions network would be sufficient to generate the correct activation of the transcription factor network in the correct spatiotemporal sequence: high caudal concentrations of FGF would promote pluripotency markers while high rostral RA concentrations of RA would promote differentiation, with cross-repressive interaction between pathways maintaining the domains separate at caudal and rostral ends of the tissue (left to right in graphs). However, if all the interactions in the network are equally moderate (Hill constants =20, **Fig 4D**) or equally strong (Hill constants =2, **Fig 4E**), then the network does not result in the proper spatial resolution of temporal states seen in wild type embryos. In both cases, transcription of the mesoderm marker *T/Bra* is not restricted to the caudal end, but instead, it is detected throughout the caudal two thirds of the tissue, partially overlapping rostrally with the

transcription of differentiation genes *Pax6* and *Ngn2* (**Fig 4D, E**). Only a subset of interaction strengths give rise to correct spatial order of identities (**Table 2; Fig 4F**). The values of the interactions strengths that generate proper spatial distribution of transcripts could be increased or decreased by about 30%, highlighting the robustness of the interaction model. These results suggest that signaling inputs encodes the information required to specify different cell maturation states, but that the transcription factor network is what determines the spatial distribution and organization of maturation states cell along the caudal-to-rostral length of the tissue.

Table 2: Hill constant for correct spatiotemporal distribution of cellular states.

Hill constants	**Description**	**Value***
F_{FT}	FGF8 dependent activation of *T*	10
F_{FS}	FGF8 dependent activation of *Sox2*	50
F_{FC}	FGF8 dependent activation of *Cdx4*	5
F_{FX}	FGF8 dependent repression of *X*	1
F_{FY}	FGF8 dependent repression of *Y*	1
W_{WN}	WNT8C dependent activation of *Nkx1.2*	10
W_{WC}	WNT8C dependent activation of *Cdx4*	10
S_{ST}	SOX2 dependent repression of *T*	2
T_{TS}	T dependent repression of *Sox2*	20
N_{NN}	NKX1.2 dependent repression of *Nkx1.2*	100
N_{NP}	NKX1.2 dependent repression of *Pax6*	20
C_{CX}	CDX4 dependent activation of *X*	10
C_{CP}	CDX4-RA complex dependent activation of *Pax6*	10
R_{RS}	RA dependent activation of *Sox2*	1
R_{RP}	RA dependent activation of *Pax6*	10
X_{XN}	X dependent repression of *Nkx1.2*	1

X_{XN2}	X dependent repression of *Ngn2*	1
P_{PY}	PAX6 dependent activation of *Y*	5
P_{PN2}	PAX6 dependent activation of *Ngn2*	20
Y_{YC}	Y dependent repression of *Cdx4*	5
*Correct spatiotemporal distribution of cellular states is also obtained when individual values are increased or decreased by 30%		

The transcription network executes the spatiotemporal information provided by the signaling factor network

To further evaluate the contribution of signaling and transcription factors networks on cell maturation events, we tested the effect of disrupting individual network nodes on transcription readouts. First, we tested the response of the transcription network to signaling noise. In simulations, both periodic disturbance (**Fig 5A**) and random noise (**Fig 5B**) were well tolerated by the transcription network without any distortions in the spatiotemporal resolution of the cellular states. This suggest that transcription network has built in robustness to extrinsic disturbances.

Fig 5. Transcription factor network responds to large, but not small, alterations in signaling information. (**A, B**) Transcription factor output is not affected by oscillatory (**A**) or random noise (**B**) in signaling inputs. Compare outputs to those obtained in Fig 4F. (**C, D**) Large changes in signaling input changes transcription factor expression domains. (**C**) Discreet (Boolean) signaling inputs. (**D**) Linear gradient signaling inputs.

Then, we evaluated the role of signaling gradients in determining the spatiotemporal resolution of downstream targets' transcriptional domains. Replacing the exponential gradient of the signaling factors with a Boolean switch (**Fig 5C**) or a linear gradients (**Fig 5D**), resulted in

loss of proper resolution of transition zones. Thus, changes in the spatial information contained in the signaling network changes the transcription network readouts. This suggests that the spatial information is encoded in the signaling and not in transcription factor network.

We previously proposed a central role of CDX4 in regulating proper maturation of NPs in the PNT. To theoretically test CDX4 role in the transcription network regulation, we evaluated the transcription profile of network genes after removing, increasing or introducing noise to *Cdx4* transcription (**Fig 6**). When *Cdx4* was removed from the simulation, *Nkx1.2* transcription expanded rostrally, overlapping significantly with the expression of differentiation markers *Pax6* and *Ngn2* (**Fig 6A**). This phenomenon is opposite to what is observed experimentally, were downregulation of CDX4 activity using an ENRCDX4 repression construct results in downregulation of *Nkx1.2* [12] (see discussion below). Conversely, when the levels of *Cdx4* were increased in the simulation, *Nkx1.2* expression domain shifted caudally, away from *Pax6* expression domain, and rostral cells did not activate the late differentiation gene *Ngn2* (**Fig 6B**). Similar results were observed experimentally [12]. Thus, removing or increasing *Cdx4* transcription affects the spatial relationship between early specification gene *Nkx1.2* and neural differentiation gene *Ngn2*, indicating that CDX4 function in the network is key to establish a transition zone between pluripotency and differentiation states. This function of CDX4 is robust, as introduction of noise in the transcription of *Cdx4* did not affect the specification of the early differentiation transition zone (**Fig 6C)**. Thus, with one exception discussed below, our simulation agree with our *in vivo* observed role of CDX4 in driving NP maturation during early spinal cord development.

Fig 6. CDX4 function is necessary for proper interpretation of signaling input by transcription factor network. (**A**) Compared to standard conditions (Fig 4D), loss of *Cdx4*

expression causes a large rostral expansion of *Nkx1.2* domain, a small reduction in *Pax6* domain and a large caudal expansion in *Ngn2* domain. These transcriptional changes results in the overlap of stem cell and differentiation genes. (**B**) Overexpression of *Cdx4* reduces *Nkx1.2* and eliminates *Ngn2* expression domains, expanding the early differentiation zone and effectively eliminating terminal cell differentiation. (**C**) Incorporation of noise into *Cdx4* transcription has insignificant effects on gene expression outputs. Loss of spatial expression is depicted by white empty rectangle and gain in spatial expression as black outlined rectangles.

Discussion

Signaling factor simulation recapitulates signaling dynamics observed in natural systems

Our simulations describe the possible behaviors the FGF8-WNT8C-RA system can exhibit under various interaction conditions (**Fig 2**). With small variations in interaction's strength, the system can model behaviors associated with different stages of axial tissue development. In a system where the FGF's activity dominates over RA's activity, the simulation most closely resembles the neural tissue at early stages of axial extension, whereas in a system where FGF activity balances that of RA, the simulation resembles the maturation of spinal cord cell that occurs during axial elongation. In contrast, a switch in the system from FGF to RA most closely resembles the processes occurring during termination of body axis extension [9, 41]. Significantly, when the interactions between FGF and RA components are weak, the system oscillates, resembling the oscillations observed between FGF/Wnt and the Notch signaling pathway during the process of paraxial mesoderm segmentation [42]. Thus, with small

modifications in signal components interaction, one can observe large changes in the behavior of the system equivalent to the changes normally observed in the spinal cord during axial elongation.

We propose a model of vertebrate body extension where modulation of interaction strength between different components of the system (e.g., transcriptionally, post-transcriptionally or epigenetically), could regulate the spatio-temporal dynamics involved in vertebrate body extension. In this model, the time at which the system transitions from FGF dominant, to FGF-RA balance, to RA switch respectively determine the time of tissue induction, elongation and termination. For example, a long period in which the FGF8-RA balance system is operational could explain the elongated axis of vertebrates such as snakes; as long as the FGF8-RA balance system remains operational, the caudal progenitor/stem cell pool will continue to generate tissue and extend the axis. In this scenario, the time at which RA takes over the system to initiate progenitor cell differentiation will determines the axial body length, with a fast FGF-RA switch resulting in a shorter body axis and vice versa.

Transcription network simulation recapitulates cell state transitions in the caudal neural plate

Results from simulation support a role for CDX in coordinating upstream signaling factors with downstream transcription network components involved in spinal cord neural maturation. In the present model, CDX4 functions to separate caudal stem cell populations (*Nkx1.2*$^{+}$ *Pax6*$^{-}$ *Ngn2*$^{-}$) and from rostral differentiating cells (*Nkx1.2*$^{-}$ *Pax6*$^{+}$ *Ngn2*$^{+}$) by establishing a transition zone. This is achieved by CDX4 repressing the stem cell gene *Nkx1.2* and the late differentiation gene

Ngn2, and by activating the early differentiation gene *Pax6*. In simulations, high levels of *Cdx4* transcription resulted in downregulation of genes repressed by CDX4 (**Fig 6B**): *Ngn2* transcription was lost while the anterior limit of *Nkx1.2* transcription shifted caudally. Only the caudal expression of *Nkx1.2* was retained due to its high dependence on WNT stimulation [35]. Increasing *Cdx4* transcription does not have a significant impact on *Pax6* expression domain as CDX4 activity on *Pax6* is under the control of RA secreted from somites [12, 38]. Together, the changes in *Nkx1.2* and *Ngn2* transcription induced by CDX4 overexpression effectively increase the size of the transition zone. The same way that premature differentiation signals has been predicted to cause shortening of the embryonic axis [31], a greater separation of stem cell and differentiation signals is predicted to cause axial lengthening. These predictions would need to be tested experimentally.

Significantly, results obtained by simulating loss of *Cdx4* activity (**Fig 6A**) did not fully match experiments done *in vivo*. With respect to differentiation genes, the network recapitulates *in vivo* results: *Pax6* transcription was not affected due to dependence of this gene on RA [12, 38], whereas *Ngn2* transcription was upregulated because this gene is normally repressed by CDX4 [12]. In contrast, with respect to the NMP marker *Nkx1.*2, loss of *Cdx4* caused an anterior expansion of *Nkx1.2* expression domain that was not observed experimentally. This discrepancy can be attributed to the use of a dominant negative form of CDX4 to downregulate its activity (ENRCDX4; [12]). Dominant-negative ENRCDX4 works by outcompeting endogenous CDX4 for binding sites in target genes to repress transcription [43], which is different than not having the CDX4 protein altogether (e. g, through a deletion of the gene). Given that our model simulates the loss of CDX4 function and not the active repression of its downstream target genes, this providing a possible explanation for the observed discrepancies between experimental

systems. It is also possible that our current understanding of the transcription factor network is incomplete. These two possible explanations are not mutually exclusive, and could be resolved with additional experiments. Notwithstanding, the proposed transcription factor network supports a key role for CDX4 in the segregation of cell states in the nascent spinal cord, providing a robust mechanisms for the progressive maturation of cells during axial elongation.

Author contributions

P.J. and I.S. designed the experiments. P.J. derived the mathematical equations, coded the simulation and performed experiments. P.J. and I.S. analyzed the results and wrote the manuscript.

Competing interests

No competing interest declared.

Acknowledgements

We thank Dr. Donald DeAngelis for guidance and for sharing his mathematical expertise, and members of the Skromne lab for intellectual discussion. We also thank Dr. K. G. Story (U Dundee, UK), Dr. M. Gouldin (Salk Institute, USA). Dr. F. Medeville (CBI, France), Dr. S. Mackem (NCI, USA), Dr. Y. Marikawa (U Hawaii, USA), Dr. A. V. Morales (Cajal Institute, Spain) and Dr. B. Novitch (UCLA, USA) for generously providing plasmids.

Funding

P. J. was supported by Sigma XI GIAR, and the University of Miami College of Art and Science Dean's summer and dissertation grants. I. S. was supported by University of Miami College of Arts and Sciences and the Neuroscience Program, and by the National Science Foundation (IOS-090449 and IOS-1755386).

References

1. Housden BE, Perrimon N. Spatial and temporal organization of signaling pathways. Trends in biochemical sciences. 2014;39(10):457-64. Epub 2014/08/27. doi: 10.1016/j.tibs.2014.07.008. PubMed PMID: 25155749; PubMed Central PMCID: PMCPMC4477539.
2. Egli D, Birkhoff G, Eggan K. Mediators of reprogramming: transcription factors and transitions through mitosis. Nature reviews Molecular cell biology. 2008;9(7):505-16. Epub 2008/06/24. doi: 10.1038/nrm2439. PubMed PMID: 18568039.
3. Basson MA. Signaling in cell differentiation and morphogenesis. Cold Spring Harbor perspectives in biology. 2012;4(6). Epub 2012/05/10. doi: 10.1101/cshperspect.a008151. PubMed PMID: 22570373; PubMed Central PMCID: PMCPMC3367549.
4. Perrimon N, Pitsouli C, Shilo BZ. Signaling mechanisms controlling cell fate and embryonic patterning. Cold Spring Harbor perspectives in biology. 2012;4(8):a005975. Epub 2012/08/03. doi: 10.1101/cshperspect.a005975. PubMed PMID: 22855721; PubMed Central PMCID: PMCPMC3405863.
5. Zaret KS, Watts J, Xu J, Wandzioch E, Smale ST, Sekiya T. Pioneer factors, genetic competence, and inductive signaling: programming liver and pancreas progenitors from the endoderm. Cold Spring Harbor symposia on quantitative biology. 2008;73:119-26. Epub 2008/11/26. doi: 10.1101/sqb.2008.73.040. PubMed PMID: 19028990; PubMed Central PMCID: PMCPMC2773436.
6. Zaret KS, Carroll JS. Pioneer transcription factors: establishing competence for gene expression. Genes & development. 2011;25(21):2227-41. Epub 2011/11/08. doi: 10.1101/gad.176826.111. PubMed PMID: 22056668; PubMed Central PMCID: PMCPMC3219227.
7. Halfon MS, Carmena A, Gisselbrecht S, Sackerson CM, Jimenez F, Baylies MK, et al. Ras pathway specificity is determined by the integration of multiple signal-activated and tissue-restricted transcription factors. Cell. 2000;103(1):63-74. Epub 2000/10/29. PubMed PMID: 11051548.
8. Henrique D, Abranches E, Verrier L, Storey KG. Neuromesodermal progenitors and the making of the spinal cord. Development (Cambridge, England). 2015;142(17):2864-75. Epub 2015/09/04. doi: 10.1242/dev.119768. PubMed PMID: 26329597.
9. Wilson V, Olivera-Martinez I, Storey KG. Stem cells, signals and vertebrate body axis extension. Development (Cambridge, England). 2009;136(10):1591-604. Epub 2009/04/28. doi: 10.1242/dev.021246. PubMed PMID: 19395637.
10. Gouti M, Metzis V, Briscoe J. The route to spinal cord cell types: a tale of signals and switches. Trends in genetics : TIG. 2015;31(6):282-9. Epub 2015/04/01. doi: 10.1016/j.tig.2015.03.001. PubMed PMID: 25823696.

11. Gouti M, Tsakiridis A, Wymeersch FJ, Huang Y, Kleinjung J, Wilson V, et al. In vitro generation of neuromesodermal progenitors reveals distinct roles for wnt signalling in the specification of spinal cord and paraxial mesoderm identity. PLoS biology. 2014;12(8):e1001937. Epub 2014/08/27. doi: 10.1371/journal.pbio.1001937. PubMed PMID: 25157815; PubMed Central PMCID: PMCPMC4144800.
12. Joshi P, Darr AJ, Skromne I. CDX4 regulates the progression of neural maturation in the spinal cord. Developmental biology. 2019. Epub 2019/03/03. doi: 10.1016/j.ydbio.2019.02.014. PubMed PMID: 30825428.
13. Diez del Corral R, Olivera-Martinez I, Goriely A, Gale E, Maden M, Storey K. Opposing FGF and retinoid pathways control ventral neural pattern, neuronal differentiation, and segmentation during body axis extension. Neuron. 2003;40(1):65-79. Epub 2003/10/07. PubMed PMID: 14527434.
14. Delfino-Machin M, Lunn JS, Breitkreuz DN, Akai J, Storey KG. Specification and maintenance of the spinal cord stem zone. Development (Cambridge, England). 2005;132(19):4273-83. Epub 2005/09/06. doi: 10.1242/dev.02009. PubMed PMID: 16141226.
15. Gouti M, Delile J, Stamataki D, Wymeersch FJ, Huang Y, Kleinjung J, et al. A Gene Regulatory Network Balances Neural and Mesoderm Specification during Vertebrate Trunk Development. Developmental cell. 2017;41(3):243-61.e7. Epub 2017/05/02. doi: 10.1016/j.devcel.2017.04.002. PubMed PMID: 28457792; PubMed Central PMCID: PMCPMC5425255.
16. Koch F, Scholze M, Wittler L, Schifferl D, Sudheer S, Grote P, et al. Antagonistic Activities of Sox2 and Brachyury Control the Fate Choice of Neuro-Mesodermal Progenitors. Developmental cell. 2017;42(5):514-26.e7. Epub 2017/08/23. doi: 10.1016/j.devcel.2017.07.021. PubMed PMID: 28826820.
17. Takemoto T, Uchikawa M, Yoshida M, Bell DM, Lovell-Badge R, Papaioannou VE, et al. Tbx6-dependent Sox2 regulation determines neural or mesodermal fate in axial stem cells. Nature. 2011;470(7334):394-8. Epub 2011/02/19. doi: 10.1038/nature09729. PubMed PMID: 21331042; PubMed Central PMCID: PMCPMC3042233.
18. Yamaguchi TP, Takada S, Yoshikawa Y, Wu N, McMahon AP. T (Brachyury) is a direct target of Wnt3a during paraxial mesoderm specification. Genes & development. 1999;13(24):3185-90. Epub 2000/01/05. doi: 10.1101/gad.13.24.3185. PubMed PMID: 10617567; PubMed Central PMCID: PMCPMC317203.
19. Herrmann BG, Labeit S, Poustka A, King TR, Lehrach H. Cloning of the T gene required in mesoderm formation in the mouse. Nature. 1990;343(6259):617-22. Epub 1990/02/15. doi: 10.1038/343617a0. PubMed PMID: 2154694.
20. Pituello F, Medevielle F, Foulquier F, Duprat AM. Activation of Pax6 depends on somitogenesis in the chick embryo cervical spinal cord. Development (Cambridge, England). 1999;126(3):587-96. Epub 1999/01/07. PubMed PMID: 9876187.
21. Diez del Corral R, Storey KG. Opposing FGF and retinoid pathways: a signalling switch that controls differentiation and patterning onset in the extending vertebrate body axis. BioEssays : news and reviews in molecular, cellular and developmental biology. 2004;26(8):857-69. Epub 2004/07/27. doi: 10.1002/bies.20080. PubMed PMID: 15273988.
22. Bel-Vialar S, Medevielle F, Pituello F. The on/off of Pax6 controls the tempo of neuronal differentiation in the developing spinal cord. Developmental biology. 2007;305(2):659-73. Epub 2007/04/03. doi: 10.1016/j.ydbio.2007.02.012. PubMed PMID: 17399698.
23. Olivera-Martinez I, Storey KG. Wnt signals provide a timing mechanism for the FGF-retinoid differentiation switch during vertebrate body axis extension. Development (Cambridge, England). 2007;134(11):2125-35. Epub 2007/05/18. doi: 10.1242/dev.000216. PubMed PMID: 17507413.
24. Sherman MS, Cohen BA. Thermodynamic state ensemble models of cis-regulation. PLoS computational biology. 2012;8(3):e1002407. Epub 2012/04/06. doi:

10.1371/journal.pcbi.1002407. PubMed PMID: 22479169; PubMed Central PMCID: PMCPMC3315449.
25. Santillan M. On the Use of the Hill Functions in Mathematical Models of Gene Regulatory Networks. MATHEMATICAL MODELLING OF NATURAL PHENOMENA. 2008;3(2):85-97. doi: 10.1051/mmnp:2008056.
26. Shi W, Ma W, Xiong L, Zhang M, Tang C. Adaptation with transcriptional regulation. Scientific reports. 2017;7:42648. Epub 2017/02/25. doi: 10.1038/srep42648. PubMed PMID: 28233824; PubMed Central PMCID: PMCPMC5324054.
27. Wilkinson DG, Nieto MA. Detection of messenger RNA by in situ hybridization to tissue sections and whole mounts. Methods in enzymology. 1993;225:361-73. Epub 1993/01/01. PubMed PMID: 8231863.
28. Lunn JS, Fishwick KJ, Halley PA, Storey KG. A spatial and temporal map of FGF/Erk1/2 activity and response repertoires in the early chick embryo. Developmental biology. 2007;302(2):536-52. Epub 2006/11/25. doi: 10.1016/j.ydbio.2006.10.014. PubMed PMID: 17123506.
29. Kumar S, Duester G. Retinoic acid controls body axis extension by directly repressing Fgf8 transcription. Development (Cambridge, England). 2014;141(15):2972-7. Epub 2014/07/24. doi: 10.1242/dev.112367. PubMed PMID: 25053430.
30. Dubrulle J, Pourquie O. fgf8 mRNA decay establishes a gradient that couples axial elongation to patterning in the vertebrate embryo. Nature. 2004;427(6973):419-22. Epub 2004/01/30. doi: 10.1038/nature02216. PubMed PMID: 14749824.
31. Olivera-Martinez I, Harada H, Halley PA, Storey KG. Loss of FGF-dependent mesoderm identity and rise of endogenous retinoid signalling determine cessation of body axis elongation. PLoS biology. 2012;10(10):e1001415. Epub 2012/11/03. doi: 10.1371/journal.pbio.1001415. PubMed PMID: 23118616; PubMed Central PMCID: PMCPmc3484059.
32. Cunningham TJ, Colas A, Duester G. Early molecular events during retinoic acid induced differentiation of neuromesodermal progenitors. Biology open. 2016;5(12):1821-33. Epub 2016/11/02. doi: 10.1242/bio.020891. PubMed PMID: 27793834; PubMed Central PMCID: PMCPMC5200905.
33. Boulet AM, Capecchi MR. Signaling by FGF4 and FGF8 is required for axial elongation of the mouse embryo. Developmental biology. 2012;371(2):235-45. Epub 2012/09/08. doi: 10.1016/j.ydbio.2012.08.017. PubMed PMID: 22954964; PubMed Central PMCID: PMCPMC3481862.
34. Bel-Vialar S, Itasaki N, Krumlauf R. Initiating Hox gene expression: in the early chick neural tube differential sensitivity to FGF and RA signaling subdivides the HoxB genes in two distinct groups. Development (Cambridge, England). 2002;129(22):5103-15. Epub 2002/10/26. PubMed PMID: 12399303.
35. Tamashiro DA, Alarcon VB, Marikawa Y. Nkx1-2 is a transcriptional repressor and is essential for the activation of Brachyury in P19 mouse embryonal carcinoma cell. Differentiation; research in biological diversity. 2012;83(5):282-92. Epub 2012/04/06. doi: 10.1016/j.diff.2012.02.010. PubMed PMID: 22475651; PubMed Central PMCID: PMCPMC3590073.
36. Takemoto T, Uchikawa M, Kamachi Y, Kondoh H. Convergence of Wnt and FGF signals in the genesis of posterior neural plate through activation of the Sox2 enhancer N-1. Development (Cambridge, England). 2006;133(2):297-306. Epub 2005/12/16. doi: 10.1242/dev.02196. PubMed PMID: 16354715.
37. Nordstrom U, Maier E, Jessell TM, Edlund T. An early role for WNT signaling in specifying neural patterns of Cdx and Hox gene expression and motor neuron subtype identity. PLoS biology. 2006;4(8):e252. Epub 2006/08/10. doi: 10.1371/journal.pbio.0040252. PubMed PMID: 16895440; PubMed Central PMCID: PMCPMC1502144.

38. Novitch BG, Wichterle H, Jessell TM, Sockanathan S. A requirement for retinoic acid-mediated transcriptional activation in ventral neural patterning and motor neuron specification. Neuron. 2003;40(1):81-95. Epub 2003/10/07. PubMed PMID: 14527435.
39. Sasai N, Kutejova E, Briscoe J. Integration of signals along orthogonal axes of the vertebrate neural tube controls progenitor competence and increases cell diversity. PLoS biology. 2014;12(7):e1001907. Epub 2014/07/16. doi: 10.1371/journal.pbio.1001907. PubMed PMID: 25026549; PubMed Central PMCID: PMCPMC4098999.
40. Pownall ME, Isaacs HV, Slack JM. Two phases of Hox gene regulation during early Xenopus development. Current biology : CB. 1998;8(11):673-6. Epub 1998/06/23. PubMed PMID: 9635197.
41. Denans N, Iimura T, Pourquie O. Hox genes control vertebrate body elongation by collinear Wnt repression. eLife. 2015;4. Epub 2015/02/27. doi: 10.7554/eLife.04379. PubMed PMID: 25719209; PubMed Central PMCID: PMCPMC4384752.
42. Oates AC, Morelli LG, Ares S. Patterning embryos with oscillations: structure, function and dynamics of the vertebrate segmentation clock. Development (Cambridge, England). 2012;139(4):625-39. Epub 2012/01/26. doi: 10.1242/dev.063735. PubMed PMID: 22274695.
43. Isaacs HV, Pownall ME, Slack JM. Regulation of Hox gene expression and posterior development by the Xenopus caudal homologue Xcad3. The EMBO journal. 1998;17(12):3413-27. Epub 1998/06/17. doi: 10.1093/emboj/17.12.3413. PubMed PMID: 9628877; PubMed Central PMCID: PMCPmc1170678.

SUPPLEMENTARY INFORMATION

Supplementary methods

Supplementary figures

Fig S1. Hill constant determine the strength of activating and repressing interactions. (A) In a system with a constant amount of activator, downstream targets with lower Hill constants (H1=1) have higher rate of production and reach higher final concentration values than targets with a higher Hill constant (H4=100). **(B)** Similar results are observed in a system with graded input of activator, except that the response of the targets is delayed. **(C)** In a system with a

constant amount of repressor, targets with lower Hill constant decline faster and to lower levels than targets with a higher Hill constant. **(D)** Similar results are observed in systems with graded input of repressor. Input is shown in blue. Outputs for the different Hill constants are shown in other colors: H1=1 in red, H2=10 in orange, H3=20 in purple, and H4=100 in green.

Fig S2. FGF-WNT-RA signaling interaction results in different stable mRNA profiles. (**A**) Profiles of mRNA transcripts at t=6000 min associated with production of signaling protein and metabolites (shown in **Fig 2C** left panels). (**B**) FGF-RA balance simulation ran for t=30,000 min, showing the stability of the profile over longer simulation time (compared to **Fig 2C** top row).

Fig S3. Aberrant RA distribution profiles in the absence of positive RA feedback. Weak positive feedback of RA on *Raldh2* production results in aberrant RA, but not FGF, distribution. (**A**) Peak of RA at the level of the field where the FGF-RA switch should occur (1500-2000 μm). (**B**) Oscillatory fluctuation of RA levels in the region of cell differentiation (>1500 μm).

APPENDIX

SIGNET.m: Matlab code for simulating signaling dynamics.

TRANSNET.m: Matlab code for simulating transcriptional factor dynamics.

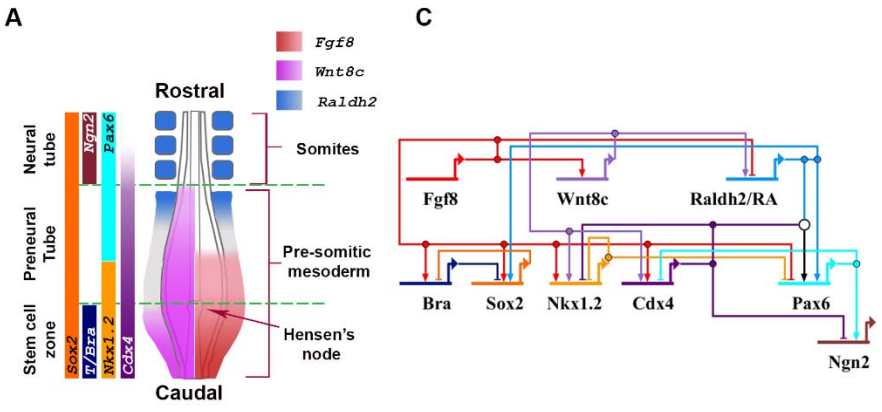

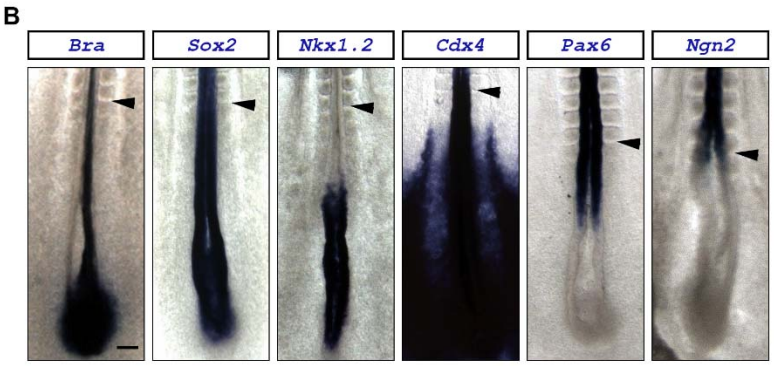

FIGURES

Figure 1

Figure 2

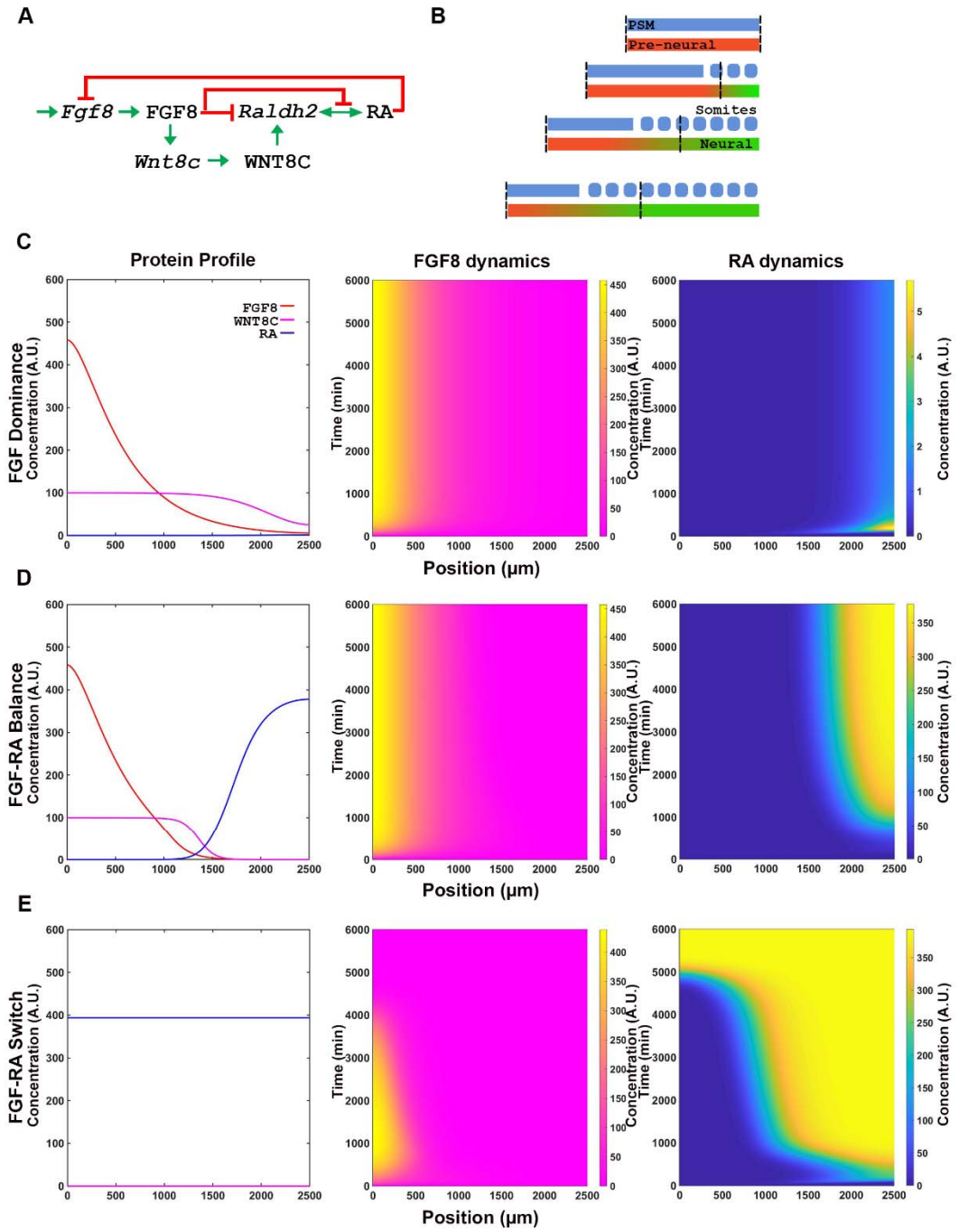

Figure 3

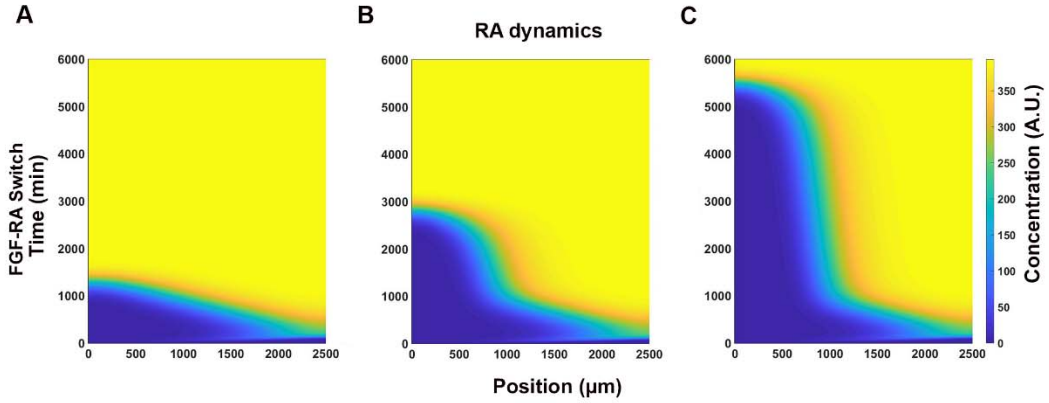

Figure 4

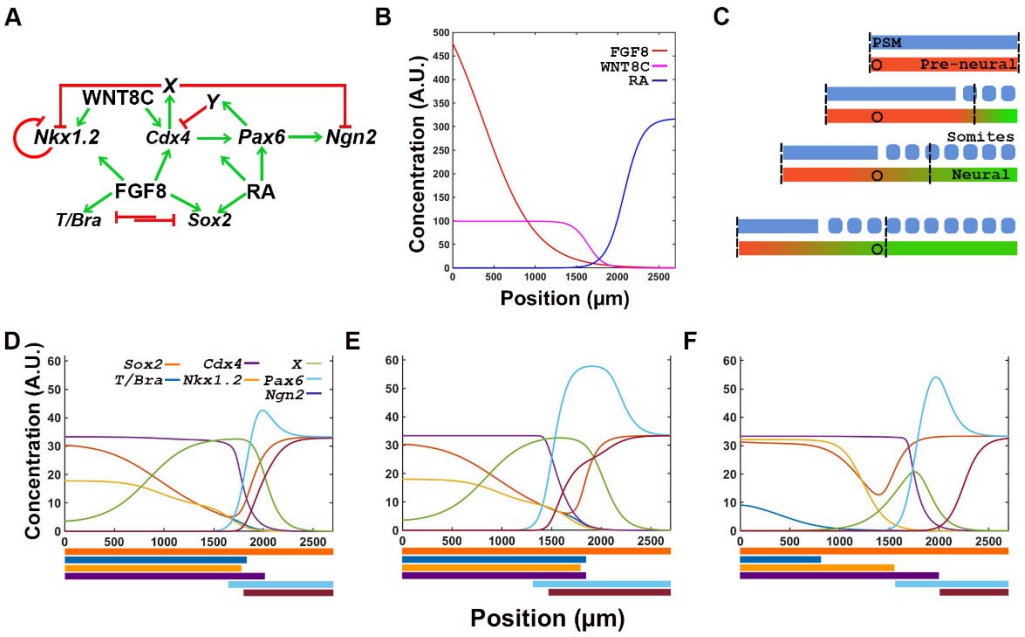

Figure 5

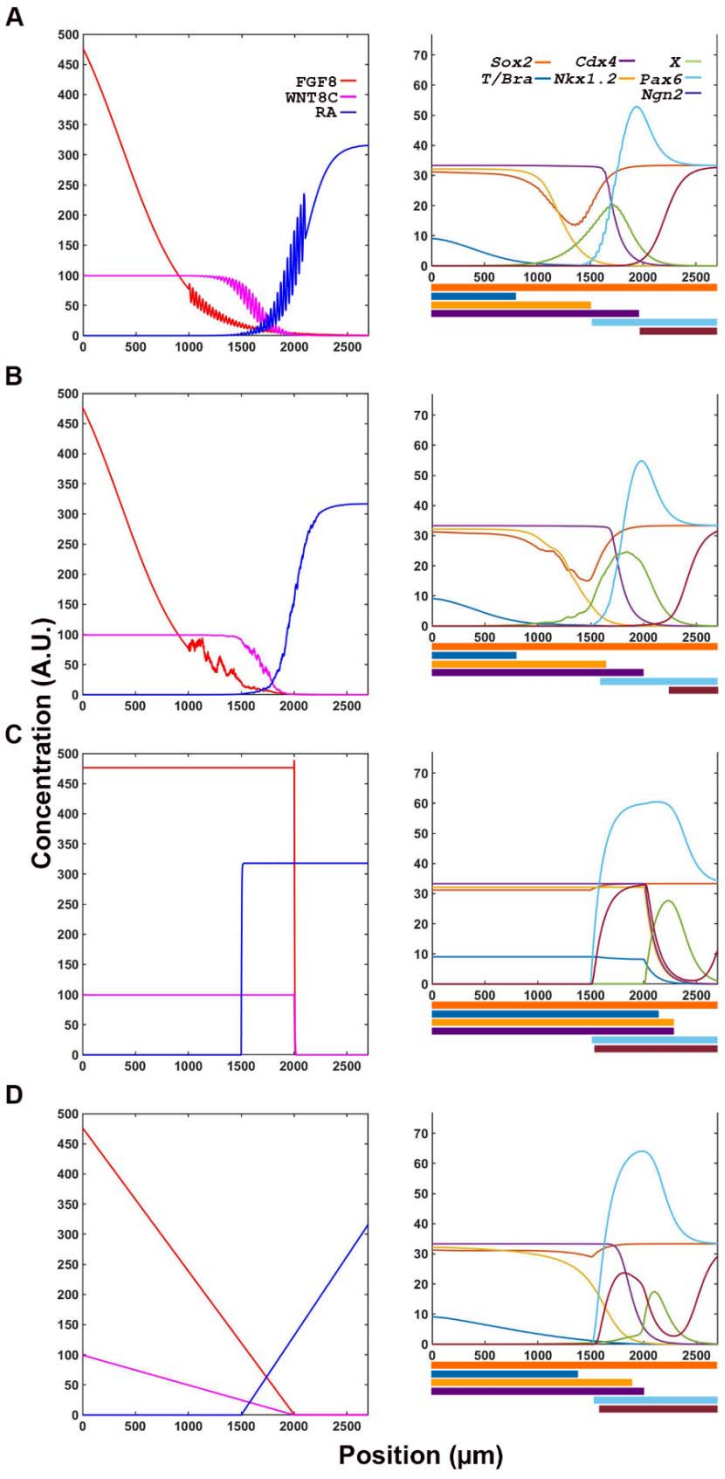

Figure 6

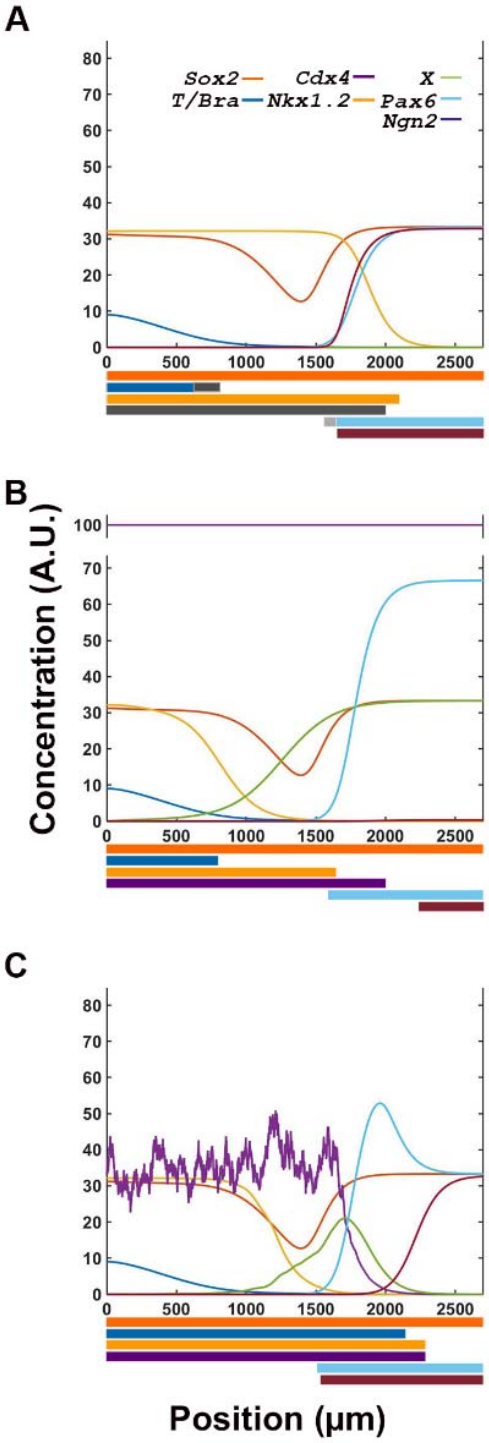

Figure S1

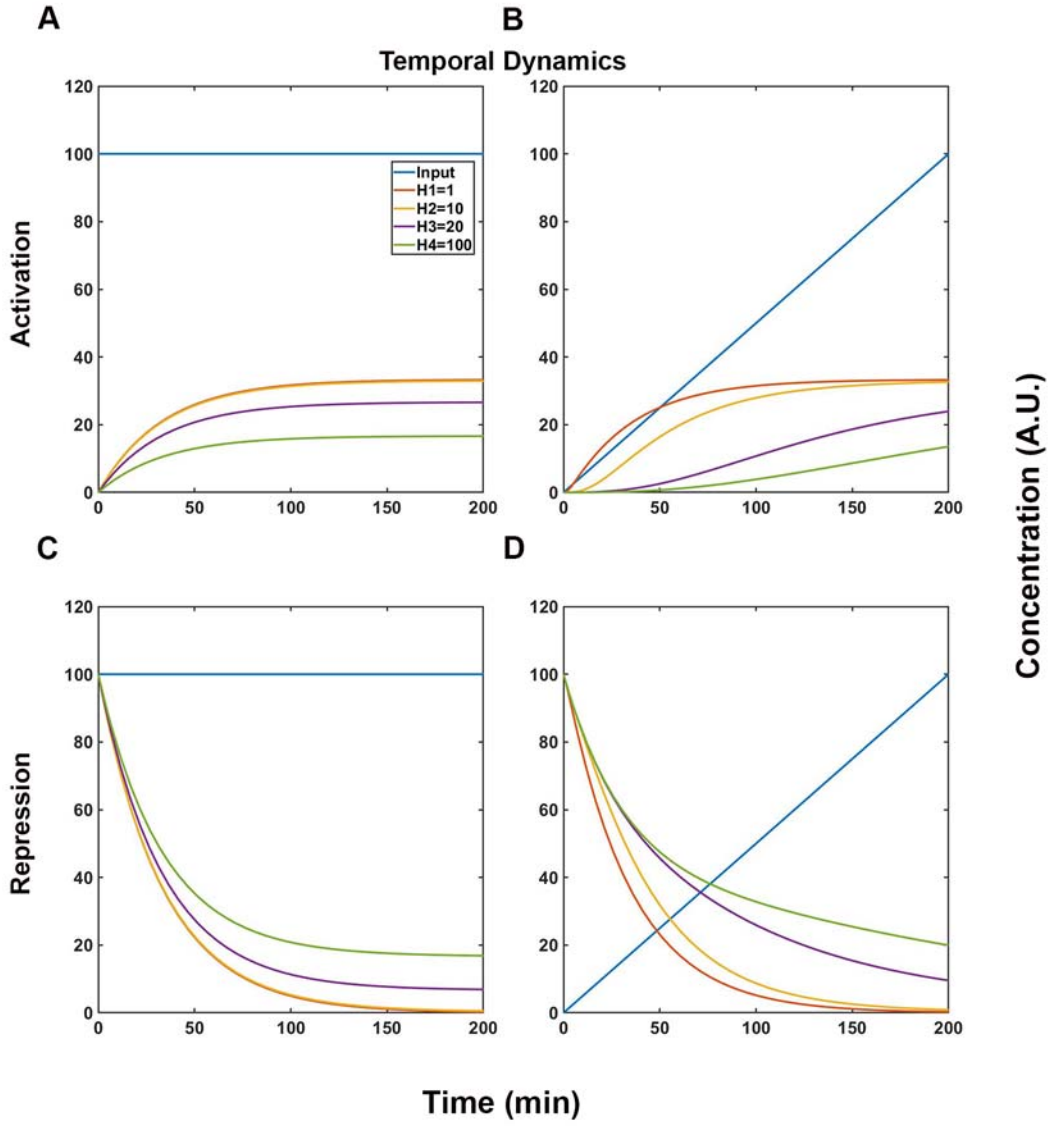

Figure S2

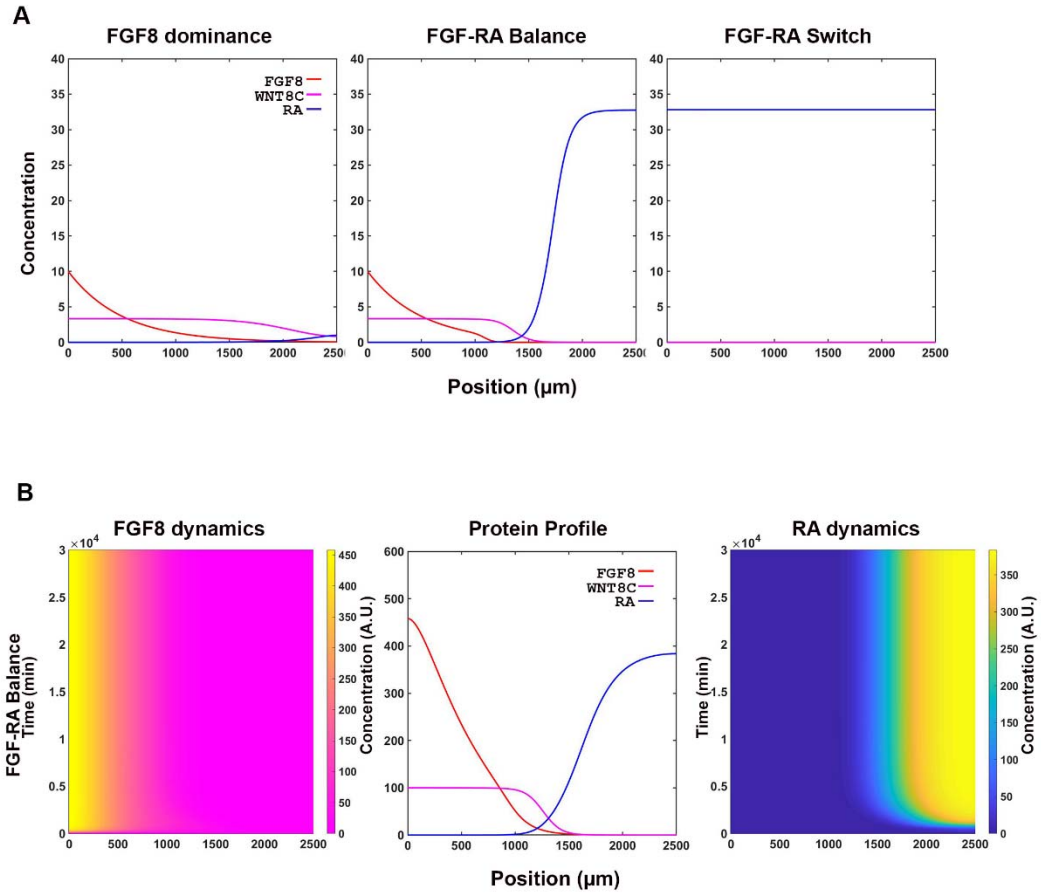

Figure S3